Multi-Criteria Approach to Inspect Line Resonance Analysis Signatures of Wind Farm Cables

(Article begins on next page)

Multi-Criteria Approach to Inspect Line Resonance Analysis Signatures of Wind Farm Cables

Gabriele Malgaroli
Dip. Energia "Galileo Ferraris"
Politecnico di Torino
Torino, Italy
gabriele.malgaroli@polito.it

Fabio Salvadori
Dip. Energia "Galileo Ferraris"
Politecnico di Torino
Torino, Italy
fabio.salvadori@polito.it

Andrea Mazza
Dip. Energia "Galileo Ferraris"
Politecnico di Torino
Torino, Italy
andrea.mazza@polito.it

Viviana R. B. Borriello
Dip. Energia "Galileo Ferraris"
Politecnico di Torino
Torino, Italy
viviana.borriello01@gmail.com

Paolo Fantoni
Department of Technology
Wirescan AS
Trollåsen, Norway
pff@wirescan.no

Filippo Norat
RES Operation Unit
CVA Eos
Châtillon, Italy
norat.filippo@cvaeos.it

Maurice Grimod
RES Operation Unit
CVA Eos
Châtillon, Italy
grimod.maurice@cvaeos.it

Abstract

Cable joints represent critical points in medium-voltage power lines, where localized impedance discontinuities may lead to faults or performance degradation. This paper proposes a multi-criteria peak detection methodology for the analysis of Line Resonance Analysis (LIRA) signatures. The approach is based on a baseline–residual decomposition, where a smooth baseline is estimated via a sparsified median-driven spline, and candidate peaks are identified using prominence and statistical significance criteria. The method is validated on measurements from a 37.95 MW wind power plant, analyzing underground cables over two campaigns (2024–2025). The algorithm detects approximately 6–10 peaks per phase in 2024 and 5–9 in 2025, with spatial repeatability within 100–200 m and amplitude variations below 5–8 dB for most events. These results indicate that the majority of detected peaks correspond to stable structural features, while only a limited subset may be associated with evolving conditions.

Index Terms

Cable diagnostics, Line Resonance Analysis, peak detection, reflectometry, fault detection, cable joints, impedance discontinuities, condition monitoring, wind power plants.

I. Introduction

The increasing penetration of renewable energy sources [1] has imposed strict requirements on the availability and reliability of power generation systems. In this context, their availability is not only determined by the intermittency of the primary energy resource (e.g., wind [2] or solar irradiance [3]), but also by the operational continuity of the electrical infrastructure composing the plant [4]. Indeed, even in the case of favorable environmental conditions, failures in electrical components can lead to significant energy losses and reduced system performance [5].

Among the elements of power generation plants, medium- and high-voltage cable systems are fundamental in ensuring the electricity transmission from the production systems to the grid connection points. Their reliability directly affects the overall plant availability, in particular in the newest installations, in which underground cable networks are widely adopted in both wind and photovoltaic applications [6], [7]. In this framework, availability can be interpreted as a combined function of both resource availability and component reliability, with particular emphasis on electrical interconnections.

Despite the key role of cable systems, the existing literature mainly focuses on general fault detection techniques and reflectometry-based methods, such as Time Domain Reflectometry (TDR) [8], [9] and Frequency Domain Reflectometry (FDR) [10], [11]. However, limited attention has been devoted to the specific role of cable joints and their impact on system-level availability. This gap is fundamental considering that joints represent intrinsic discontinuities in the cable structure, where electrical, thermal, and mechanical properties may vary significantly from those of the bulk cable [12].

Cable joints introduce localized impedance variations that can evolve over time due to factors like dielectric inhomogeneity, mechanical stress, moisture, or assembly issues [13]. These variations may lead to partial reflections, increased losses, and eventually localized defects or failures, whose detection is, generally, difficult in their early stages using conventional diagnostic techniques. Specifically, experimental studies show that often impedance discontinuities and anomalous reflections are related to joint locations, confirming their critical role within cables [14]. In particular, recent measurement campaigns have demonstrated that the most significant anomalies in cable signatures are often concentrated at joint positions, where maintenance actions or external stresses tend to modify significantly the electrical response of the line [15].

Furthermore, field observations indicate that incorrect maintenance activities and external mechanical interventions can damage the structure of the cables by introducing new defects even in previously healthy sections, with a consequent variation

Presented at the 26th International Conference on Environment and Electrical Engineering and the 10th Industrial and Commercial Power Systems Europe, Lisbon (Portugal), 29th June - 2nd July 2026.

of the electrical behavior of the joints. This highlights not only the vulnerability of these components but also the need for advanced diagnostic tools capable of detecting variations in their electrical characteristics over time.

This work aims to address this gap by proposing focusing on the diagnosis and characterization of cable joint behavior through advanced reflectometric techniques, with the objective of improving fault detection capabilities and supporting predictive maintenance strategies in modern power generation plants. Specifically, this paper investigates measurements performed using the Line Resonance Analysis (LIRA) [16]–[19] system in a 37.95 MW wind power plant installed in Southern Italy. The pipelines installed between the HV/MV substation and the MV/LV substation (length of about 16 km) are analyzed, addressing the most important faults in the joints of the cable system.

The paper is organized as follows: Section II introduces the LIRA system in comparison with conventional TDR and FDR techniques. Section III presents the power generation plant and the cable system under analysis, while Section IV offers the results of the analysis. Finally, Section V contains the conclusions of the work.

II. Methods for Fault Detection using Time-Domain and Frequency-Domain Approaches

A. Theoretical Background

The Line Resonance Analysis (LIRA) method operates in the frequency domain and is based on the evaluation of the complex input impedance spectrum of a cable over a wide frequency band. The goal is the determination of the spatial distribution of impedance discontinuities (e.g., joints, defects) from the measured frequency response [20].

B. Input Impedance Determination

The LIRA injects in the cable a voltage signal with N values of variable frequency f_{k} depending on the length of the cable [21]. For each frequency, the input voltage ($V_{\text{in}}(f_{\text{k}})$) and current ($I_{\text{in}}(f_{\text{k}})$) are measured and the corresponding input frequency $Z_{\text{in}}(f_{\text{k}})$ is computed with Ohm's Law [22] and the impedance spectrum $Z_{\text{in}}(f)$ containing the complete propagation and reflection behaviour of the cable is achieved [23]:

$$Z_{in}(f) = Z_{in}(f_k)_{k=1}^{N} = |Z_{in}(f)|e^{j\phi(f)} \tag{1}$$

C. Mathematical Modeling of Transmission Line Propagation

The general transmission-line solution is the superposition of a forward-propagating wave and a reflected wave [24]. Therefore, the voltage and current phasors are defined as:

$$\frac{d^2V(z)}{dz^2} = (R + j\omega L)(G + j\omega C)V(z) \tag{2}$$

$$\frac{d^2I(z)}{dz^2} = (R + j\omega L)(G + j\omega C)I(z) \tag{3}$$

The solution of the equations is the following:

$$\widetilde{V}(x) = V^+e^{-\gamma x} + V^-e^{+\gamma x} \tag{4}$$

$$\widetilde{I}(x) = I^+e^{-\gamma x} + I^-e^{+\gamma x} \tag{5}$$

where V^+ and I^+ are the voltage and current amplitudes of the forward wave, while V^- and I^- are the amplitudes of the reflected wave. The complex propagation constant γ consists of the the attenuation constant α and the phase constant β, which is the derivative of the phase ϕ with respect to position x, as follows:

$$\gamma = \alpha + j\beta \tag{6}$$

D. Mathematical Analysis of Propagation Delay and Phase Variation

When a propagating waveform meets a defect in the cable at the position x_{i}, the signal flows back to the input of the cable and the distance is $2x_{\text{i}}$.

The contribution of a discontinuity at a position x_{i} can be expressed as follows:

$$e^{-2\gamma(f)x_i} = e^{-2\alpha(f)x_i}e^{-j2\beta(f)x_i} \tag{7}$$

The amplitude term $e^{-2\alpha(f)x_i}$ accounts for attenuation and depends on multiple factors, including propagation losses, reflection magnitude, and measurement conditions. On the contrary, the phase term $e^{-j2\beta(f)x_i}$ encodes the propagation delay and provides a direct estimation for the position of the discontinuity. Indeed, the phase constant β is a function of the frequency as:

$$\beta(f) = \frac{\omega}{v_{\text{p}}} = \frac{2\pi f}{v_{\text{p}}} \tag{8}$$

where v_{p} is the phase velocity.

Substituting into the phase term:

$$e^{-j2\beta(f)x_i} = e^{-j2\left(\frac{2\pi f}{v_p}\right)x_i} = e^{-j\frac{4\pi f x_i}{v_p}} \tag{9}$$

Defining the round-trip delay:

$$\tau_i = \frac{2x_i}{v_p} \tag{10}$$

the phase term becomes:

$$e^{-j2\beta(f)x_i} = e^{-j2\pi f \tau_i} \tag{11}$$

The expression $e^{-j2\pi f \tau_i}$ corresponds to a pure time delay in the frequency domain. Therefore, each discontinuity located at x_i introduces a delayed component characterized by τ_i.

This establishes a direct relationship between the position and the frequency-dependent phase variation.

In the presence of multiple reflections, the measured signal can be approximated as:

$$\Gamma(f) \approx \sum_i A_i(f) e^{-j2\pi f \tau_i} \tag{12}$$

where $A_i(f)$ includes both reflection coefficients and attenuation effects.

E. Spatial Estimation and Signature Computation

The spatial information is retrieved by transforming the signal into the delay domain using the inverse Fourier transform:

$$\Gamma(\tau) = \mathcal{F}^{-1}\Gamma(f) \tag{13}$$

Each term $e^{-j2\pi f \tau_i}$ produces a peak at τ_i, allowing the estimation of the position x_i. The phase velocity v_p is estimated using a proprietary algorithm by LIRA.

$$x_\mathrm{i} = \frac{v_\mathrm{p}\tau_\mathrm{i}}{2} \tag{14}$$

Finally, the LIRA provides a graphical representation of the signature, which is computed in the following way:

$$S(x) = 20\log_{10}|\Gamma(x)| \tag{15}$$

To assess whether a peak is significant, the signal is analyzed locally with an algorithm different from that implemented in LIRA.

F. Peak Selection Methodology

Peak detection in signatures is performed through a baseline–residual decomposition followed by a statistically and physically constrained selection criterion.

Let $y(x)$ denote the measured signature as a function of distance x. A smooth baseline $b(x)$ is estimated using a sparsified cubic spline interpolation of locally computed median values, in order to suppress narrow peaks and high-frequency oscillations. The residual signal is then defined as:

$$r(x) = y(x) - b(x) \tag{16}$$

Candidate peaks are identified on $r(x)$ using a prominence-based criterion. A point x_i is considered a peak if its prominence P_i satisfies the following condition:

$$P_i \geq \max\left(\alpha \cdot \sigma_r,\, P_{\min}\right) \tag{17}$$

where σ_r is a robust estimate of the residual noise level computed via the Median Absolute Deviation (MAD),

$$\sigma_r = 1.4826 \cdot \mathrm{median}\left(|r(x) - \mathrm{median}(r(x))|\right) \tag{18}$$

α is a scaling factor, and $P_{\min}$ is a minimum absolute prominence threshold. Additionally, a minimum spatial separation $\Delta x_{\min}$ between peaks is enforced to avoid multiple detections of the same physical feature.

For each detected peak at position x_i, a local background region $\mathcal{B}_i$ is defined as:

$$\mathcal{B}_i = \{x \mid |x - x_i| \leq L_c\} \setminus \bigcup_j \{x \mid |x - x_j| \leq L_g\}\,, \tag{19}$$

where L_c is the context half-width and L_g is the guard interval around each detected peak. This range ensures that the background estimation is not contaminated by neighbouring peaks.

Within $\mathcal{B}_i$, the local background statistics are computed as:

$$\mu_i = \mathrm{mean}\left(y(x)\right), \quad \sigma_i = \mathrm{std}\left(y(x)\right), \tag{20}$$

and analogously for the residual signal:

$$\mu_{r,i} = \text{mean}\left(r(x)\right), \quad \sigma_{r,i} = \text{std}\left(r(x)\right). \tag{21}$$

The peak significance is then quantified through both raw and residual contrasts:

$$C_i = y(x_i) - \mu_i, \quad C_{r,i} = r(x_i) - \mu_{r,i}, \tag{22}$$

and corresponding normalized scores:

$$Z_i = \frac{C_i}{\sigma_i}, \quad Z_{r,i} = \frac{C_{r,i}}{\sigma_{r,i}}. \tag{23}$$

A peak is classified as a potential fault if it satisfies the following combined criteria:

$$\begin{cases} P_i \geq P_{\min}, \\ Z_{r,i} \geq Z_{\text{th}}, \\ C_i \geq C_{\text{th}}, \\ y(x_i) \geq y_{\text{th}}, \end{cases} \tag{24}$$

where Z_{th}, C_{th}, and y_{th} are predefined thresholds on residual significance, local contrast, and absolute signal level, respectively.

This multi-criteria selection framework enables the rejection of spurious local maxima caused by structural oscillations or measurement noise, while preserving peaks that are both statistically significant and physically consistent with fault-induced reflections along the cable.

G. Comparison with TDR and FDR Techniques

The LIRA method can be included in the frame of reflectometry-based diagnosis techniques, specifically the Time Domain Reflectometry (TDR) and the Frequency Domain Reflectometry (FDR). These classes of methods rely on the analysis of reflected signals generated by impedance discontinuities; however, factors like the excitation strategy, the signal processing, the sensitivity, and the diagnostic capabilities might differ significantly [23].

1) Time Domain Reflectometry (TDR): TDR operates by injecting a fast voltage pulse into the cable and observing the reflected waveform in the time domain [25]. The time delay between the incident and reflected signals is directly proportional to the distance of the impedance discontinuity, allowing direct fault localization. However, TDR presents the following limitations:

- Limited sensitivity with low changes of distributed parameters.
- Constrained spatial resolution by hardware and signal attenuation.
- Strong attenuation effects in long or lossy cables.
- Poor performance with gradual or global aging phenomena.

2) Frequency Domain Reflectometry (FDR): FDR injects sinusoidal signals over a frequency sweep and analyzes the reflected signal as a function of frequency [26]. Similarly to LIRA, the localization of defects is obtained through an inverse transformation. With respect to TDR, the FDR approach offers a higher resolution due to a fine control of the bandwith, and improved noise robustness thanks to the application of averaging and filtering techniques.

However, conventional FDR techniques rely on the analysis of the reflection coefficient magnitude, neglecting part of the phase information. This results in:

- Reduced sensitivity to small dielectric variations,
- Limited capability to detect early-stage degradation,
- Weaker discrimination between local and global effects.

The LIRA method extends the FDR concept by exploiting the full complex impedance spectrum, including both magnitude and phase information, and by leveraging resonance phenomena as a sensitivity enhancement mechanism. In particular, LIRA can be considered an advanced evolution of FDR, combining spectral analysis, resonance amplification, and complex signal processing to overcome the intrinsic limitations of conventional reflectometry techniques [27].

III. Case study

This paper proposes an innovative procedure for the early detection of faults and degradation in cable joints within power generation plants. Specifically, the Line Resonance Analysis (LIRA) method was applied to the MV/HV substation of the Monteverde wind power plant (Avellino, Italy). Two different experimental campaigns were conducted, in 2024 and 2025. The first campaign identified many joints with critical states of health along the lines connecting the wind turbine generators to the secondary substation, which were subsequently replaced. Then, follow-up measurements were carried out in 2025 to monitor the remaining assets and validate the long-term integrity and criticality threshold of the cable joints. Nevertheless, the state of health of replaced joints in 2024 were investigated by Centro Elettrotecnico Sperimentale Italiano (CESI), which confirmed the results obtained by the LIRA proprietary algorithm.

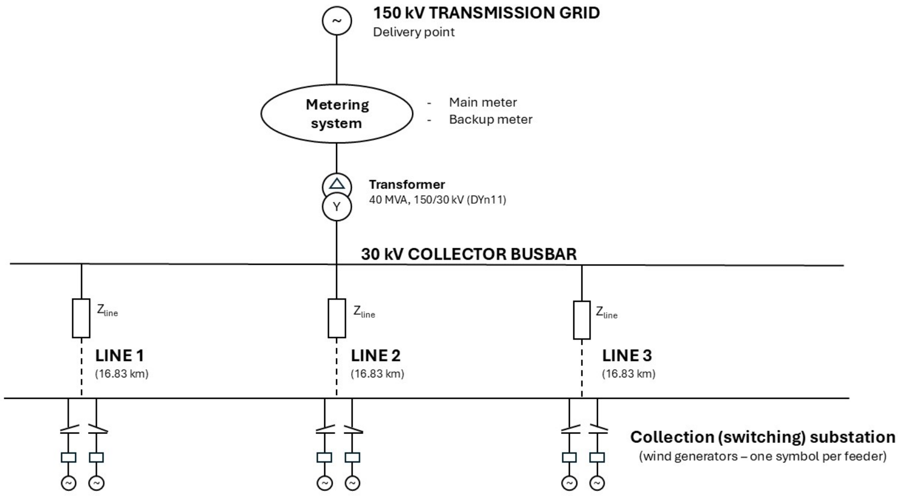

Fig. 1: Single line diagram of the Monteverde Wind Farm (37.95 MW).

A. *Wind power plant description*

The wind farm consists of 11 wind turbines with rated power of 3.45 MW each, specifically three Vestas V112 units and eight Vestas V117 units. The total installed capacity of the plant is 37.95 MW, with an estimated average yearly energy production of about 73 GWh. The plant was installed in 2018 in Monteverde due to its favourable wind conditions, and it is currently managed by the CVA S.p.A. group.

The electrical structure of the plant is the following (scheme in Fig. 1):

- Each wind turbine is connected to a synchronous generator and a transformer, increasing the voltage from 0.75 kV to 30 kV. Then, underground pipelines connect the generators with the switching substation.
- A switching substation collects the electricity generated by the wind turbines of the plant (rated voltage of 30 kV). This substation includes the cable terminations form the turbines, and the related protection devices (switches, fuses and disconnectors) for each underground power line.
- A MV/HV substation permits the connection to the electricity grid (rated voltage of 150 kV), including a three-phase transformer with rated power of 40 MVA. The switching substation is connected to the primary substation through three underground pipelines with a length of 16.83 km each.

B. *Measurement method and connections*

The electrical connection of the LIRA device to the power lines under test is the following. The LIRA device includes a red and a black terminal, which are connected to the phase terminal of the single-core cables (red terminal) and to a single-core grounding cable, which aggregates the shield grounds of the three phases (black terminal). The measurement consists of two stages, the first performed in the primary substation and the second performed in the switching substation. Prior to the device connection, the grounding of the surge protection devices was disconnected to prevent current paths during the measurement. Moreover, the High Voltage (HV) transformer was disconnected to avoid background noise.

IV. Results and Discussion

This section details the experimental results of the analysis. The proposed peak detection methodology was applied to multiple LIRA signatures acquired in two consecutive measurement campaigns (2024 and 2025). Representative results for the three phases of a line are shown from Fig. 2 to Fig. 4, where the raw signatures (blue and green curves for 2024 and 2025 data, respectively) are compared with the corresponding spline-based baselines (orange and red curves for 2024 and 2025 data, respectively) and the detected peak locations.

The baseline estimation, based on a sparsified median-driven cubic spline, effectively captures the large-scale attenuation trend of the cable while suppressing high-frequency oscillations. The adopted smoothing configuration ensures that the baseline follows variations occurring over distances larger than approximately $500\text{–}800\,\mathrm{m}$, thus preserving localized discontinuities in the residual signal.

Peak detection was performed using a combined criterion based on prominence, residual-based statistical significance, and local contrast. In particular, peaks were required to satisfy a minimum prominence $P_{\min}$ in the range of $20\,\mathrm{dB}$ and a residual z-score threshold $Z_{\mathrm{th}} > 3.5$. A minimum spatial separation $\Delta x_{\min}$ of approximately $300\text{–}500\,\mathrm{m}$ was enforced to avoid multiple detections of the same physical feature. From a quantitative standpoint, the algorithm detected between $N_{2024} \approx 6\text{–}10$ peaks per phase in the 2024 dataset and $N_{2025} \approx 5\text{–}9$ peaks per phase in the 2025 dataset. The majority of these peaks exhibit a spatial alignment between the two campaigns within a tolerance of approximately $100\text{–}200\,\mathrm{m}$, indicating that they correspond to persistent structural features of the cable, such as joints or known impedance discontinuities.

The difference in peak amplitude between the two campaigns is generally limited, with variations typically below $5\text{–}8\,\mathrm{dB}$ for aligned peaks. This further supports the interpretation that most detected events are stable over time. A limited number of peaks exhibit larger amplitude deviations or appear only in one of the two datasets. These cases, characterized by either a significant change in prominence or the absence of spatial correspondence, may indicate potential evolving conditions or measurement variability. However, their occurrence remains sparse compared to the total number of detected peaks.

Overall, the results confirm that the proposed methodology is effective in identifying a consistent set of dominant reflections, with good repeatability across measurement campaigns. At the same time, the quantitative analysis highlights that most detected peaks are associated with persistent cable features rather than transient faults. This observation underscores a fundamental limitation of single-acquisition analysis and motivates the integration of multi-temporal comparison strategies to enhance fault discrimination capability.

V. Conclusions

A multi-criteria peak detection methodology for LIRA signature analysis has been presented and validated on real measurements from a 37.95 MW wind power plant. The proposed approach combines spline-based baseline estimation with residual analysis and statistical peak selection. The method demonstrated stable performance across different measurement campaigns, detecting approximately 6–10 peaks per phase in 2024 and 5–9 in 2025. A spatial repeatability within 100–200 m was observed for most peaks, while amplitude variations remained below 5–8 dB, confirming the robustness of the detection process. Dominant peaks exhibited contrasts typically above 20 dB, whereas secondary detections were characterized by lower amplitudes and reduced significance. The results indicate that most detected peaks are associated with persistent structural features, such as cable joints, while only a limited number of events show significant variations between campaigns. This confirms the effectiveness of the proposed method in isolating physically meaningful reflections, while also highlighting the intrinsic limitation of single-acquisition analysis in distinguishing faults from stable discontinuities. Future developments will focus on integrating multi-temporal comparison and topology-aware criteria to improve fault discrimination and support predictive maintenance strategies.

References

[1] F. Spertino, G. Malgaroli, A. Amato, M. Qureshi, A. Ciocia, and H. Siddiqi, "An innovative technique for energy assessment of a highly efficient photovoltaic module," *Solar*, vol. 2, pp. 377–389, 2022.

[2] D. Astolfi, G. Malgaroli, F. Spertino, A. Amato, A. Lombardi, and L. Terzi, "Long term wind turbine performance analysis through scada data: A case study," in *2021 IEEE 6th International Forum on Research and Technology for Society and Industry (RTSI)*, 2021, pp. 7–12.

[3] A. Ciocia, D. Enescu, A. Amato, G. Malgaroli, R. Polacco, F. Amico, and F. Spertino, "Agrivoltaic system: a case study of pv production and olive cultivation in southern italy," in *2022 57th International Universities Power Engineering Conference (UPEC)*, 2022, pp. 1–6.

[4] F. Spertino, E. Chiodo, A. Ciocia, G. Malgaroli, and A. Ratclif, "Maintenance Activity, Reliability Analysis and Related Energy Losses in Five Operating Photovoltaic Plants," in *Proceedings - 2019 IEEE International Conference on Environment and Electrical Engineering and 2019 IEEE Industrial and Commercial Power Systems Europe, EEEIC/I and CPS Europe 2019*, 2019.

[5] M. Arifujjaman, M. Iqbal, and J. Quaicoe, "Reliability analysis of grid connected small wind turbine power electronics," *Applied Energy*, vol. 86, no. 9, pp. 1617–1623, 2009.

[6] CIGRE Working Group B1.66, "Recommendations for Testing DC Lapped Cable Systems for Power Transmission at a Rated Voltage up to and Including 800 kV," CIGRE, Tech. Rep. Technical Brochure 853, 2021, eLECTRA, No. 319, December 2021. [Online]. Available: https://electra.cigre.org/319-december-2021/technical-brochures/recommendations-for-testing-dc-lapped-cable-systems-for-power-transmission-at-a-rated-voltage-up-to-and-including-800-kv.html

[7] J. Tao, S. U. Rehman, R. Ali, and S. A. Raza, "Advancement and challenges: A review of power cable aging monitoring and diagnostic techniques," *Renewable and Sustainable Energy Reviews*, vol. 222, p. 115970, 2025.

[8] P. Smith, C. Furse, and J. Gunther, "Analysis of spread spectrum time domain reflectometry for wire fault location," *IEEE Sensors Journal*, vol. 5, no. 6, pp. 1469–1478, 2005.

[9] T.-W. Pan, C.-W. Hsue, and J.-F. Huang, "Time-domain reflectometry using arbitrary incident waveforms," *IEEE Transactions on Microwave Theory and Techniques*, vol. 50, no. 11, pp. 2558–2563, 2002.

[10] H. Vanhamme, "High resolution frequency-domain reflectometry," *IEEE Transactions on Instrumentation and Measurement*, vol. 39, no. 2, pp. 369–375, 1990.

[11] C. Furse, Y. Chung, C. Lo, and P. Pendayala, "A critical comparison of reflectometry methods for location of wiring faults," *Smart Structures and Systems*, vol. 2, 01 2006.

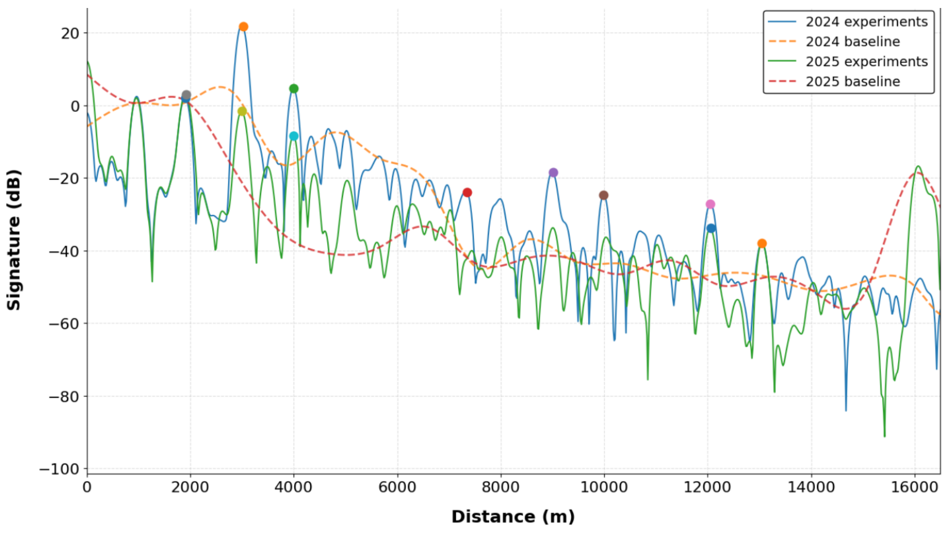

Fig. 2: Signature and baseline profiles for phase #1 of the line under analysis.

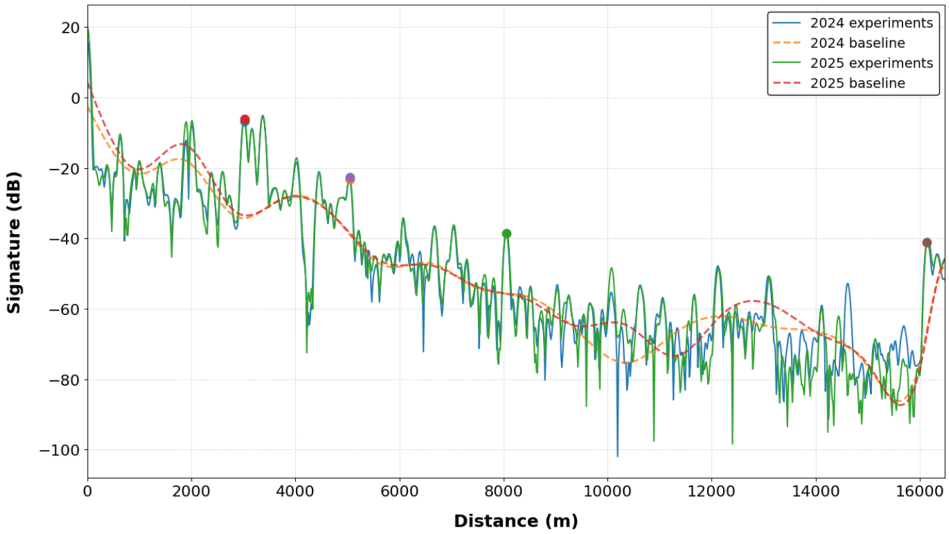

Fig. 3: Signature and baseline profiles for phase #2 of the line under analysis.

[12] L. Anghelescu, A. D. Handra, and B. M. Diaconu, "Degradation Pathways of Electrical Cable Insulation: A Review of Aging Mechanisms and Fire Hazards," *Fire*, vol. 8, no. 10, 2025.

[13] M. AlShaikh Saleh, A. N. Alquennah, A. Ghrayeb, S. S. Refaat, H. Abu-Rub, and S. P. Khatri, "A Review on the Lifetime Estimation Methods of XLPE Power Cables," *IEEE Open Journal of Industry Applications*, vol. 6, pp. 445–489, 2025.

[14] B. Diban, G. Mazzanti, and R. E. Diaz, "Life Estimation of HVDC Extruded Cables Subjected to Extension of Qualification Test Conditions and Comparison with Prequalification Test Conditions," *Energies*, vol. 18, no. 14, 2025.

[15] Q. Shi, U. Troeltzsch, and O. Kanoun, "Detection and localization of cable faults by time and frequency domain measurements," in *2010 7th International Multi- Conference on Systems, Signals and Devices*, 2010, pp. 1–6.

[16] P. Fantoni, "Advancements in wire condition monitoring using line impedance resonance analysis (lira)," in *International Conference on Condition Monitoring, Diagnosis and Maintenance (CMDM) 2015*, 10 October 2015, pp. 1–8.

[17] P. Fantoni and A. Manet, "Advancements in Condition Monitoring of Electrical Cables in NPP's Using Line Resonance Analysis (LIRA)," in *OECD EHPG Conference, Norway*, May 2017.

[18] P. Fantoni and G. Toman, "Condition Monitoring of Electrical Cables Using Line Resonance Analysis (LIRA)," in *6th International Topical Meeting on Nuclear Plant Instrumentation Control and Human Machine Interface Technology (NPIC&HMIT 2009)*, April 2009.

[19] P. Fantoni, "Condition Monitoring of Electrical Cables Using Line Resonance Analysis (LIRA)," in *Proceedings of ICONE17 International Conference on Nuclear Engineering*, Brussels, Belgium, Jul. 2009.

[20] P. Romano, A. Imburgia, G. Ala, E. Francomano, and F. Viola, "Condition Assessment of Low Voltage Cables via Line Resonance Analysis," in *2021 IEEE International Conference on Environment and Electrical Engineering and 2021 IEEE Industrial and Commercial Power Systems Europe (EEEIC / I&CPS Europe)*, 2021, pp. 1–5.

[21] P. Fantoni, "Advancements in Wire Condition Monitoring of Electrical Cables in NPP's Using Line Resonance Analysis (LIRA)," in *Proceedings of ICONE24 24th International Conference on Nuclear Engineering 2016*, July 2016.

[22] T. Maier, D. Lick, and T. Leibfried, "Frequency-Domain Cable Model with a Real Representation of Joints and Smooth Failure Changes and a Diagnostic Investigation with Line Resonance Analysis," in *2018 Condition Monitoring and Diagnosis (CMD)*, 2018, pp. 1–6.

[23] W. Zhu, B. Hui, J. Li, T. Han, L. Zhao, and S. Hou, "Frequency Domain Reflectometry for Power Cable Defect Localization: A Comparative Study of FFT and IFFT Methods," *Energies*, vol. 18, no. 20, 2025. [Online]. Available: https://www.mdpi.com/1996-1073/18/20/5346

[24] C. R. Paul, *Analysis of Multiconductor Transmission Lines*, 1st ed. USA: John Wiley & Sons, Inc., 1994.

[25] Y. Liu, L. Peng, S. Wen, S. Li, and Z. Huang, "A Time-Frequency Domain Reflectometry for Locating Cable Insulation Damage Based on An Optimal Kernel Function Design," in *2024 Academic Conference of China Instrument and Control Society (ACCIS)*, 2024, pp. 744–749.

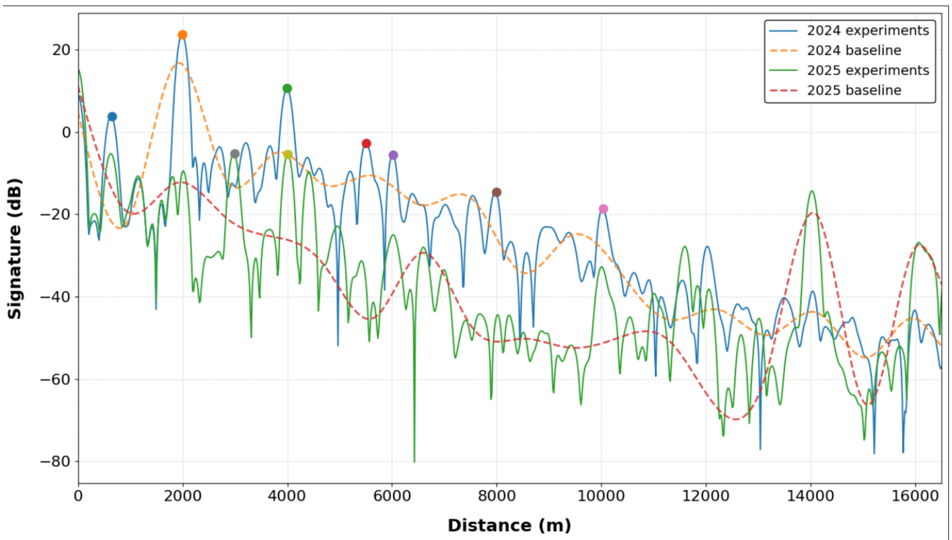

Fig. 4: Signature and baseline profiles for phase #3 of the line under analysis.

[26] H. Zhang, H. Mu, X. Zou, D. Zhang, G. Zhang, and C. Xie, "A Novel Method for Identifying Cable Defect and Improving Location Accuracy Based on Frequency Domain Reflectometry," in *2021 IEEE 4th International Electrical and Energy Conference (CIEEC)*, 2021, pp. 1–5.

[27] Q. Wan, Y. Li, R. Yuan, Q. Meng, and X. Li, "Fault Identification and Localization of a TimeFrequency Domain Joint Impedance Spectrum of Cables Based on Deep Belief Networks," *Sensors*, vol. 23, no. 2, 2023. [Online]. Available: https://www.mdpi.com/1424-8220/23/2/684